J. Membrane Biol. 213, 165–174 (2006)
DOI: 10.1007/s00232-006-0062-x

The Journal of
Membrane
Biology

Regulation of Basolateral Cl^- Channels in Airway Epithelial Cells: The Role of Nitric Oxide

Valentin Duta[1], Florentina Duta[2], Lakshmi Puttagunta[3], A. Dean Befus[2], Marek Duszyk[1]
[1]Department of Physiology, University of Alberta, Edmonton AB, T6G 2H7, Canada
[2]Department of Medicine, University of Alberta, Edmonton AB, T6G 2H7, Canada
[3]Department of Laboratory Medicine and Pathology, University of Alberta, Edmonton AB, T6G 2H7, Canada

Received: 9 August 2006/Revised: 13 October 2006

Abstract. The presence of basolateral Cl^- channels in airway epithelium has been reported in several studies, but little is known about their role in the regulation of anion secretion. The purpose of this study was to characterize regulation of these channels by nitric oxide (NO) in Calu-3 cells. Transepithelial measurements revealed that NO donors activated a basolateral Cl^- conductance sensitive to 4,4′-diisothiocyanatostilbene-2,2′-disulfonic acid (DIDS) and anthracene-9-carboxylic acid. Apical membrane permeabilization studies confirmed the basolateral localization of NO-activated Cl^- channels. Experiments using 8-bromo cyclic guanosine monophosphate (8Br-cGMP) and selective inhibitors of soluble guanylyl cyclase and inducible NO synthase (1H-[1, 2, 4] oxadiazolol-[4, 3-a] quinoxalin-1-one [ODQ] and 1400W [N-(3-Aminomethyl)benzyl)acetamidine], respectively) demonstrated that NO activated Cl^- channels via a cGMP-dependent pathway. Anion replacement and $^{36}Cl^-$ flux studies showed that NO affected both Cl^- and HCO_3^- secretion. Two different types of Cl^- channels are known to be present in the basolateral membrane of epithelial cells: Zn^{2+}-sensitive ClC-2 and DIDS-sensitive bestrophin channels. *S*-Nitrosoglutathione (GSNO) activated Cl^- conductance in the presence of Zn^{2+} ions, indicating that ClC-2 channel function was not affected by GSNO. In contrast, DIDS completely inhibited GSNO-activated Cl^- conductance. Bestrophin immunoprecipitation studies showed that under control conditions bestrophin channels were not phosphorylated but became phosphorylated after GSNO treatment. The presence of bestrophin in airway epithelia was confirmed using immunohistochemistry. We conclude that basolateral Cl^- channels play a major role in the NO-dependent regulation of anion secretion in Calu-3 cells.

Key words: Bestrophin — Bicarbonate — Cl^- flux — ClC-2

Correspondence to: Marek Duszyk; email: marek.duszyk@ualberta.ca

Introduction

Under normal conditions, the airway epithelium functions as a highly selective barrier that protects the lungs from potentially harmful substances. To facilitate this task, the epithelium has developed a number of protective mechanisms that include changes in transepithelial ion transport and altered mucociliary clearance. Anion secretion provides a driving force for hydration of the airway surface liquid. This process is coordinated by a polarized network of channels, transporters and energy-dependent pumps that are selectively expressed in the apical and/or basolateral aspects of the epithelium. In airway epithelial cells, the primary basolateral entry pathways for Cl^- and HCO_3^- are the Na^+-K^+-$2Cl^-$ (NKCC1) and the Na^+-HCO_3^- cotransporters, respectively. Both anions leave the cell via the apical Cl^- channel, the cystic fibrosis transmembrane conductance regulator (CFTR) (Devor et al., 1999).

While apical membrane Cl^- channels have been studied intensively and much is known about their role in transepithelial anion transport, the basolateral Cl^- channels have received significantly less attention. The presence of basolateral Cl^- channels in the airway epithelium was first reported over 15 years ago (Willumsen, Davis & Boucher, 1989), but little is known about their role in transepithelial anion secretion (Hwang et al., 2000). The fact that inhibition of these channels increases Cl^- secretion indicates that at least some of the Cl^- ions that enter the cell via NKCC1 cotransport are recycled across the

basolateral membrane (Szkotak, Man & Duszyk, 2003).

Presently, at least two different types of Cl^- channels have been identified in the basolateral membrane of epithelial cells: ClC-2 and bestrophin. ClC-2 Cl^- channels are broadly expressed, insensitive to 4,4′-diisothiocyanatostilbene-2,2′-disulfonic acid (DIDS) and activated by hyperpolarization, cell swelling and acidic pH (Jentsch et al., 2002). In addition to the basolateral membrane localization (Catalan et al., 2004), ClC-2 channels are present in the apical membrane (Murray, Chu & Zeitlin, 1996) and at the apical junctional complexes in epithelial cells (Gyomorey et al., 2000). Several physiological functions have been proposed for ClC-2 (Jentsch et al., 2002), but their role in transepithelial ion transport in the human airway remains unknown.

Bestrophin was initially identified as the protein product of the gene responsible for autosomal dominant vitelliform macular dystrophy (VMD), also known as Best's disease (Petrukhin et al., 1998; Marquardt et al., 1998). VMD is associated with an irregular electrooculogram, thought to reflect changes in the retinal pigment epithelium (RPE) basolateral membrane Cl^- conductance (Gallemore, Hughes & Miller, 1997). Although bestrophin mRNA and protein are highly enriched in the RPE (Petrukhin et al., 1998), this channel is also present in other epithelia, including airway epithelial cells (Duta et al., 2004). Current models of bestrophin topology suggest that this protein consists of either four (Sun et al., 2002; Petrukhin et al., 1998) or six (Qu, Fischmeister & Hartzell, 2004) transmembrane-spanning α-helices and a large C-terminal cytoplasmic region containing three potential phosphorylation sites for protein kinase A (PKA) and for cyclic guanosine monophosphate (cGMP)-dependent protein kinase (PKG) (Blom, Gammeltoft & Brunak, 1999). The fact that basolateral Cl^- channels could be activated via cyclic adenosine monophosphate (cAMP)- and/or cGMP-dependent phosphorylation (Duta et al., 2004) suggests that bestrophin could play a major role in the regulation of transepithelial anion secretion in human airways.

Activation of the nitric oxide (NO)/cGMP-dependent pathway is known to stimulate anion secretion in the human airway (Duszyk, 2001) and lung epithelial cells (Kamosinska et al., 1997). Presently, two anion channels are known to be regulated via the NO/cGMP-dependent pathway, CFTR (Seidler et al., 1997) and ICln (Furst et al., 2005). NO is produced by three NO synthases (NOS), but current evidence indicates that the respiratory tract NO is produced mainly by inducible NOS (iNOS), with little contribution from endothelial and neuronal isoforms (Lane et al., 2004). Moreover, iNOS expression can be upregulated manyfold by inflammatory agents such as cytokines, leading to generation of large amounts of NO in the airways (Asano et al., 1994). Therefore, we investigated the effects of endogenous and cytokine-induced NO on transepithelial Cl^- secretion. Our results indicate that Calu-3 cells primarily secrete HCO_3^- when stimulated via the NO/cGMP pathway and that Cl^- secretion can be stimulated by blocking basolateral Cl^- channels. We also show that bestrophin Cl^- channels are broadly expressed in the human lung, not only in airway epithelial cells but also in alveolar macrophages, endothelial cells and airway smooth muscle cells.

Methods

Cells

Calu-3 cells were obtained from the American Tissue Culture Collection (Rockville, MD) and grown as described previously (Szkotak et al., 2003). Briefly, cells were maintained in T-75 flasks (Costar, Cambridge, MA) and typically required 6–8 days to reach ~85% confluence. At this time, the cells were seeded at a density of 3.5 x $10^5/cm^2$ onto Costar Snapwell inserts (0.45 μm pore size, 1 cm^2 surface area) for short-circuit current (I_{sc}) measurements and maintained in a cell culture medium containing 20% fetal bovine serum. For the first 6 days, cells were grown submerged in culture medium. Subsequently, air-liquid interface culturing was used, in which the medium was added only to the basolateral side of the inserts. Inserts were used for experiments 10-16 days after the establishment of an air-liquid interface.

Transepithelial Measurements

Cells grown on inserts were bathed on their apical and basolateral sides with 10 ml of Krebs-Henseleit solution (KHS) containing (mM) 116 NaCl, 4.7 KCl, 2.5 $CaCl_2$, 1.2 $MgCl_2$, 24.8 $NaHCO_3$, 1.2 KH_2PO_4 and 11.1 glucose (pH 7.4). Solutions were warmed to 37°C and continually circulated with a gas lift using either 95% O_2-5% CO_2 if the solution was HCO_3^--buffered or air if the solution was 4-(2-hydroxyethyl)-1-piperazineethanesulfonic acid (HEPES)-buffered. In experiments requiring HCO_3^--free KHS, the composition was (mM) 135.8 NaCl, 4.7 KCl, 2.5 $CaCl_2$, 1.2 $MgCl_2$, 1.2 KH_2PO_4, 11.1 glucose and 10 HEPES (pH 7.4). In low-Cl^- solution, NaCl (116 mM) was replaced by Na gluconate (112 mM) and $CaCl_2$ (2.5 mM) was replaced by Ca gluconate (5 mM) to compensate for the Ca^{2+}-buffering capacity of gluconate. The transepithelial potential difference was clamped to zero using a DVC 1000 amplifier (World Precision Instruments, Sarasota, FL), and the resulting I_{sc} was recorded through Ag-AgCl electrodes and 3 M KCl agar bridges. I_{sc} was sampled at 10 Hz using a PowerLab 8SP series data acquisition converter and Chart software, both from ADInstruments (Castle Hill, Australia). Brief (1 s) pulses of 0.5 m*V* were applied every 90 s, to calculate resistance. All values are expressed as an average (I_{sc}, which was calculated as the mean change in current in the first 300 s after drug addition, unless otherwise noted. During all experiments, the I_{sc} was allowed to stabilize for 20 min prior to treatments.

Polyacrylamide Gel Electrophoresis and Western Blotting

Polyacrylamide gel electrophoresis and Western blotting were carried out as described previously (Sanders & Parker, 2002). Briefly, cells were homogenized in protease inhibitor buffer containing 15 μg/ml aprotinin, 1 μg/ml leupeptin, 5 μg/ml pepsta-

tin and 1.74 mg/ml phenylmethyl sulfonyl fluoride. Protein concentration was determined using the Bio-Rad (Richmond, CA) Bradford-based protein assay method, and 50 μg of protein was added to each well of a 10% polyacrylamide gel. Proteins were transferred from the gels onto a supported nitrocellulose membrane at 100 *V* for 2 h. For immunoblotting, membrane blocking was carried out using 5% skimmed milk in Tris-buffered saline with 0.1% Tween-20 (TBS-T). Primary antibodies were incubated overnight at 4°C, followed by four washes for 10 min each, after which the peroxidase-conjugated secondary anti-rabbit immunoglobulin G (IgG; Jackson ImmunoResearch Labs, West Grove, PA) was used in a dilution of 1/10,000 in TBS-T for 1 h at room temperature. Proteins were visualized by adding enhanced chemiluminescence (ECL) Western blotting detection reagent for 10 s and then exposing the blot to Hyperfilm ECL (Amersham, Baie, Canada). Where appropriate, preabsorption controls were carried out, using the control blocking peptide supplied with the antibody. Preabsorption abolished staining in all cases (*not shown*). Controls were also carried out in which the primary antibody was replaced with normal rabbit serum; these were also negative (*not shown*). A minimum of three runs was carried out, and a representative example is shown.

Immunoprecipitation was performed with cell extracts collected in modified radioimmunoprecipitation assay buffer (Upstate Biotechnology, Waltham, MA). The cell lysate was precleared on protein A sepharose beads (Sigma, St. Louis, MO) at 4°C for 15 min, and then 0.5 mg of protein was incubated with bestrophin antibody for 2 h, followed by incubation with protein sepharose A beads overnight. The next day, the beads were washed three times with phosphate-buffered saline (PBS) and the immuno-complexes recovered by boiling with 30 μl 2x sodium dodecyl sulfate buffer containing 5% β-mercaptoethanol. The samples were analyzed by Western blot and probed with antibody that recognizes serine-, threonine- and tyrosine-phosphorylated proteins.

Radioisotopic Flux

Calu-3 inserts were short-circuited for 20 min prior to addition of the radioisotope. At time zero (T_0), background samples were taken, followed by addition of 3 μCi of $^{36}Cl^-$ (Amersham Pharmacia Biotech, Aylesbury, UK) to the basolateral compartment; another 20 min was allowed, to establish equilibrium. At this time (T_{20}), 0.5-ml samples were taken from the apical side and replaced with fresh KHS; this was repeated at 10-min intervals thereafter. Three samples were taken (T_{20}, T_{30} and T_{40}) before addition of *S*-nitrosoglutathione (GSNO, 100 μM); this was followed by two more samples (T_{50} and T_{60}) taken before addition of basolateral DIDS (50 μM) and a further two samples (T_{70} and T_{80}) taken after DIDS treatment. Two samples were also taken from the basolateral side before treatment with GSNO, to calculate the specific activity. Samples were counted in a liquid scintillation counter, and the basolateral-to-apical flux (J^{Cl}_{BA}) was calculated according to a standard equation (Schultz & Zalusky, 1964). $^{36}Cl^-$ fluxes in the apical-to-basolateral (J^{Cl}_{AB}) direction were measured in exactly the same fashion, except that the radioisotope was added to the apical bathing solution. Net $^{36}Cl^-$ flux (J^{Cl}_{net}) was calculated as $J^{Cl}_{net} = J^{Cl}_{BA} - J^{Cl}_{AB}$.

Immunohistochemistry

Human lung histopathological material was obtained from the University of Alberta Hospital, (Edmonton, Canada). The tissue used was a surgical specimen, representing visually normal lung. The study was approved by the Health Research Ethics Board, University of Alberta. After fixation, lung tissue was embedded in paraffin and sectioned at 4 μm. All steps were performed at room temperature in a humidified container to prevent tissue dehydration. Sections were deparaffinized and rehydrated, and endogenous peroxidase was blocked with 30% H_2O_2-methanol (1:4, vol/vol) for 10 min. Goat serum (Vector, Burlingame, CA) was used to block nonspecific binding, and a previously optimized concentration of primary antibody (51 μg/ml, Bestrophin E6-6, sc-32792; Santa Cruz Biotechnology, Santa Cruz, CA) in antibody diluent (Dako, Carpinteria, CA) was immediately applied to the sections and incubated for 45 min. Unbound antibody was removed by three washes in PBS. Biotinylated anti-mouse IgG (H + L) (Vector) secondary antibody (5 μg/ml) was applied to each section for 30 min, followed by 20-min incubation with horseradish peroxidase streptavidin (Vector). Slides were washed in PBS, stained with 3,3′-diaminobenzidine chromogene (Biogenex, San Ramon, CA) for 5 min and counterstained in Harris hematoxylin (Sigma). Sections were dehydrated through an alcohol series and xylene and mounted in Cytoseal XYL mounting medium (Richard-Allan Sciences, Kalamazoo, MI). Antibody localization was detected by brown staining. As negative controls, we used the same dilution of purified mouse IgG (Cedarlane, Hornby, Canada).

Chemicals

Stock solutions of DIDS (5 mM), N^G-nitro-L-arginine methyl ester (L-NAME, 100 mM), GSNO (100 mM), 8-bromine (8Br)-cGMP (50 mM) and amiloride (10 mM) were prepared in H_2O. H-89 (5 mM) was dissolved in 50% ethanol, anthracene-9-carboxylic acid (9-AC, 10 mM) in 0.1 N NaOH and 1400W [N-(3-Aminomethyl)benzyl)acetamidine] (10 mM) in methanol. 1H-(1,2,4)oxadiazolol-(4,3-a)quinoxalin-1-one (ODQ, 10 mM), KT5823 (1 mg/ml) and nystatin (90 mg/ml) were prepared in dimethyl sulfoxide. Ouabain (10 mM) was prepared in KHS. L-NAME and ODQ were purchased from Alexis Biochemicals (San Diego, CA), DIDS from Molecular Probes (Eugene, OR), KT5823 and 1400W from Calbiochem (San Diego, CA) and all other chemicals from Sigma. Goat polyclonal antibestrophin (C-14: sc-22027) and rabbit polyclonal anti-iNOS (H-174: sc-8310) antibodies were purchased from Santa Cruz Biotechnology. Antiphosphoserine/threonine/tyrosine mouse monoclonal antibody (ab15556) was purchased from Abcam (Cambridge, MA). Recombinant human cytokines interleukin 1β (IL-1β, tumor necrosis factor α (TNFα) and interferon γ (IFNγ) were purchased from Chemicon (Temecula, CA) and reconstituted in PBS according to the manufacturer's instructions.

Data Analysis

Data are presented as means ± standard error of the mean (SEM), unless otherwise indicated; *n* refers to the number of experiments. The paired Student's *t*-test was used to compare the means of two groups. Statistically significant differences among the means of multiple groups were determined by one-way analysis of variance (ANOVA) with the Tukey-Kramer posttest using Graphpad Instat 3.05 software (San Diego, CA). $P < 0.05$ was considered statistically significant.

Results

NO Activates Basolateral, DIDS-Sensitive Cl^- Channels

In total, we evaluated 58 inserts bathed in normal KHS and 24 inserts in either Cl^- or HCO_3^- free KHS. The basal I_{sc} and R_T in KHS averaged

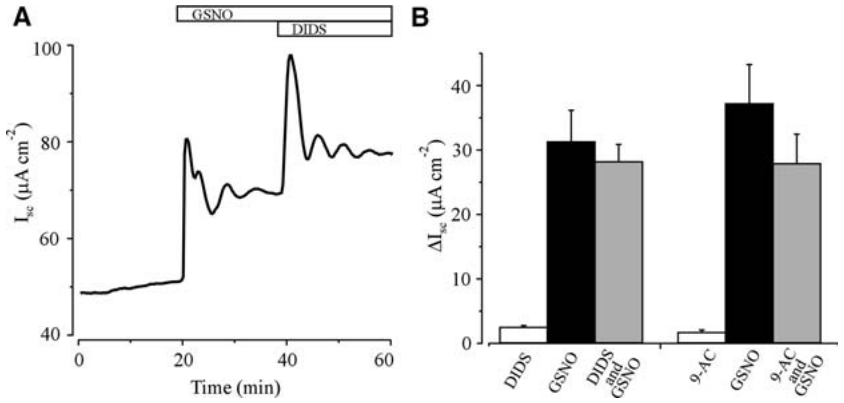

Fig. 1. The effect of GSNO and Cl^- channel blockers on I_{sc}. (*A*) Representative recording showing activation of I_{sc} by GSNO (100 μM, bilateral) and basolateral DIDS (50 μM, $n = 14$). (*B*) A bar chart showing averaged peak δI_{sc} activated by DIDS and 9-AC (1 mM, basolateral, $n = 4$) in the absence and presence of GSNO. Addition of DIDS to the basolateral side caused a small but significant increase in baseline I_{sc} ($P < 0.05$) and a much larger increase in cells pretreated with GSNO ($P < 0.0001$).

29.3 ± 4.1 μA · cm^{-2} (range 2–61 μA · cm^{-2}) and 396 ± 18 Ω/cm^2 (range 241–826 Ω/cm^2), respectively. The NO donor GSNO (100 μM, bilateral) increased peak I_{sc} by 32.5 ± 2.5 μA · cm^{-2} (range 21–48 μA · cm^{-2}, $n = 19$). Similar results were obtained with another, biochemically different NO donor, *S*-nitroso-*N*-acetyl-D,L-penicillamine (SNAP, 100 μM, $n = 3$), whereas a carrier of NO in GSNO (glutathione [GSH] 100 μM, $n = 4$) had no effect on I_{sc}. Consistent with previous findings (Szkotak et al., 2003), the absence or presence of amiloride (10 μM, apical) had no effect on I_{sc}, indicating that epithelial Na^+ channels do not contribute to the I_{sc} in Calu-3 cells.

A blocker of Cl^- transport, DIDS (50 μM), added to the apical side did not affect either baseline or GSNO-stimulated I_{sc} ($n = 6$). Basolateral DIDS caused a small but significant increase in baseline I_{sc} (2.4 ± 0.3 μA · cm^{-2}, $n = 6$, $P < 0.05$) and a much larger increase in cells pretreated with GSNO (28.1 ± 1.6 μA · cm^{-2}, $n = 14$). Figure 1A shows a typical I_{sc} recording in the presence of GSNO and basolateral DIDS. Similar results were obtained with another Cl^- transport blocker, 9-AC (1 mM, $n = 4$, Fig. 1B). These results suggest that the NO-activated, DIDS- and 9-AC-sensitive Cl^- channels are present in the basolateral membrane.

A direct measurement of the basolateral membrane Cl^- conductance was performed using apical membrane permeabilization by nystatin (90 μg/ml). The experiments were performed in the presence of ouabain (1 mM, basolateral) to inhibit Na^+/K^+-ATPase and in HCO_3^-free KHS to eliminate contribution of a Na^+-HCO_3^- cotransporter. Figure 2A shows typical current recordings in apically permeabilized Calu-3 cells, subjected to a voltage staircase of −8 to +8 m*V*. The current at the beginning and end of each trace, when *V* was 0, is the I_{sc}. The GSNO-activated current was calculated by subtracting the baseline current from the current recorded in the presence of GSNO, and the corresponding current-voltage (*I-V*) relationship is shown (Fig. 2B). The basolateral membrane conductance was determined as the slope of the *I-V* curve at 0 m*V*. GSNO-activated basolateral conductance was equal to 1.58 ± 0.06 mS · cm^{-2} ($n = 3$). Subsequent application of basolateral DIDS (50 μM) reduced this value to 0.26 ± 0.02 mS · cm^{-2}, indicating that ~84% of GSNO-activated basolateral conductance was DIDS-sensitive.

ClC−2 Cl^- channels, insensitive to DIDS but blocked by Zn^{2+} ions, have been previously identified in the basolateral membrane of colonic epithelial (Catalan et al., 2004) and in Calu−3 (Mummery, Killey & Linsdell, 2005) cells. We investigated their contribution to basolateral membrane Cl^- conductance by applying $ZnCl_2$ (50 μM, basolateral) in apically permeabilized Calu-3 cells. Zn^{2+} ions decreased basolateral membrane Cl^- conductance by 0.21 ± 0.04 mS · cm^{-2} ($n = 4$). In the presence of Zn^{2+} ions, GSNO increased the conductance by 1.49 ± 0.12 mS · cm^{-2}, indicating that channels activated by GSNO were Zn^{2+}-insensitive.

NO Stimulates Cl^- but not HCO_3^- Conductance in the Basolateral Membrane

Figure 3 shows typical I_{sc} responses to GSNO and DIDS in HCO_3^- or Cl^- free solution. In HCO_3^-free solution, GSNO increased I_{sc} by 20.9 ± 4.1 μA · cm^{-2} ($n = 4$) and subsequent application of DIDS further increased I_{sc} by 30.9 ± 0.9 μA · cm^{-2} (Fig. 3A). This indicates that DIDS prevents Cl^- recycling across the basolateral membrane, leading to enhanced Cl^- secretion across the apical membrane.

In contrast, in Cl^- free solution, GSNO increased I_{sc} by 34.8 ± 2.6 μA · cm^{-2} ($n = 4$), whereas DIDS decreased I_{sc} by 4.6 ± 1.2 μA · cm^{-2} ($n = 4$), probably due to its effects on basolateral Na^+-HCO_3^- cotransport (Fig. 3B). These results also indicate that basolateral Cl^- channels are impermeable to HCO_3^- anions.

In both solutions, addition of a selective inhibitor of soluble guanylyl cyclase, ODQ (20 μM, bilateral), brought the GSNO-activated I_{sc} to baseline levels, indicating that NO increased I_{sc} via a cGMP-dependent pathway (Fig. 3A,B).

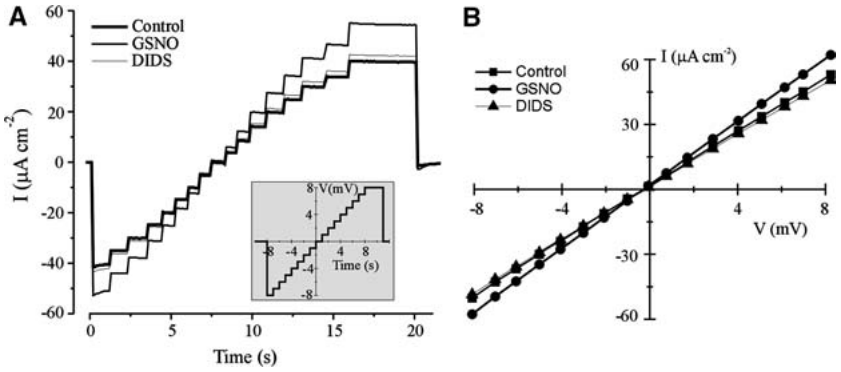

Fig. 2. GSNO activates basolateral Cl^- conductance in apically permeabilized Calu-3 cells, which is DIDS-sensitive. (*A*) Typical traces showing transepithelial current response to a voltage staircase of −8 to +8 m*V* in 1-m*V* steps. Cells were bathed in HCO_3^--free KHS bubbled with air, and the apical membrane was permeabilized with nystatin (90 μg/ml). The *inset* shows the voltage protocol used. (*B*) Current-voltage relationships under control conditions, in the presence of GSNO and DIDS ($n = 3$ in each set). The standard errors varied between 3.1 and 6.8 $\mu A \cdot cm^{-2}$ at ±8 m*V* (*not shown*).

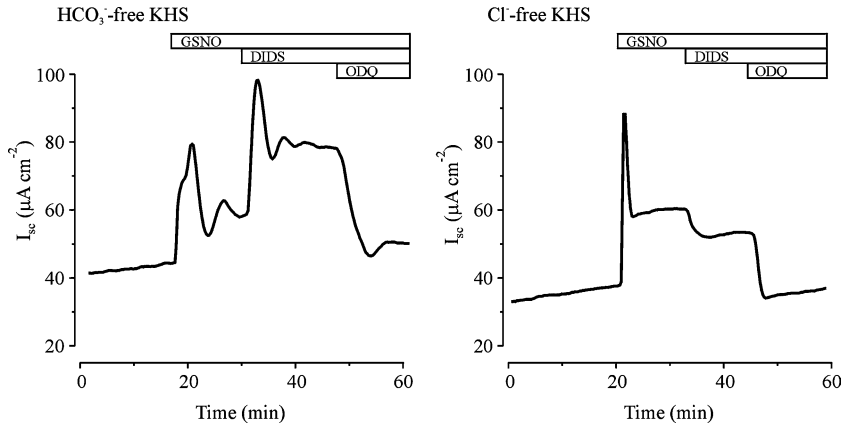

Fig. 3. The effect of GSNO on I_{sc} in HCO_3^- and Cl^- free solutions. Representative recordings showing activation of I_{sc} by GSNO (100 μM, bilateral) in (*A*) HCO_3^- free and (*B*) Cl^- free solutions, followed by DIDS (50 μM, basolateral) and ODQ (20 μM, bilateral).

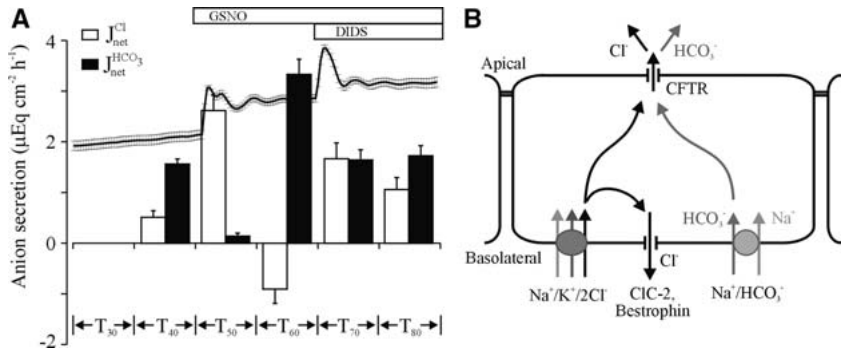

Fig. 4. (*A*) Simultaneous $^{36}Cl^-$ flux and I_{sc} measurements show the relative contributions of HCO_3^- and Cl^- to Calu−3 anion secretion. The data are expressed as a mean ± SEM ($n = 8$). The sampling periods for radioisotopic flux measurements are shown as T_X (where X is the time in minutes). Measured $^{36}Cl^-$ net flux ($J^{Cl}_{net} = J^{Cl}_{BA} - J^{Cl}_{AB}$) and calculated HCO_3^- flux ($J^{HCO3}_{net} = I_{sc} - J^{Cl}_{net}$) are shown for each sampling period. (*B*) A model of transepithelial anion secretion in airway epithelial cells.

Measurement of $^{36}Cl^-$ Secretion Reveals Cl^- Recycling across the Basolateral Membrane

Simultaneous measurements of I_{sc} and $^{36}Cl^-$ flux were performed in KHS. Figure 4 shows the averaged I_{sc} traces ($n = 8$), the net $^{36}Cl^-$ flux (J^{Cl}_{net}) and the calculated net HCO_3^- flux (J^{HCO3}_{net}) during each sample interval. The unilateral $^{36}Cl^-$ flux data are shown in Table 1. These data show that the majority of baseline I_{sc} is due to HCO_3^- secretion (T_{30}), with a smaller contribution from Cl^- ions. Application of GSNO (100 μM) stimulates transient Cl^- secretion (Fig. 4, T_{40}), followed by sustained HCO_3^- secretion (Fig. 4, T_{50}) and reduced J^{Cl}_{Net} (Table 1, T_{50}). Subsequent measurement of $^{36}Cl^-$ flux revealed that DIDS increases J^{Cl}_{Net} by increasing J^{Cl}_{BA} and decreasing Cl^- back-flux (J^{Cl}_{AB}) across the basolateral membrane (T_{60} and T_{70}, Fig. 4 and Table 1).

A schematic diagram of anion transport in airway epithelial cells may help to better understand the

Table 1. Flux and I_{sc}values

Sample	Treatment	$J^{Cl}{}_{BA}$	$J^{Cl}{}_{AB}$	$J^{Cl}{}_{net}$	I_{sc}	$J^{HCO3}{}_{net}$
T_{40}	Baseline	1.38 ± 0.25	0.87 ± 0.05	0.51 ± 0.13	2.08 ± 0.12	1.56 ± 0.12
T_{50}	GSNO	4.16 ± 0.59	1.59 ± 0.11	2.62 ± 0.30	2.76 ± 0.14	0.14 ± 0.15
T_{60}	GSNO	1.40 ± 0.54	2.30 ± 0.15	−0.90 ± 0.28	2.43 ± 0.15	3.33 ± 0.25
T_{70}	+DIDS	2.63 ± 0.58	0.96 ± 0.23	1.67 ± 0.31	3.32 ± 0.18	1.64 ± 0.21
T_{80}	+DIDS	2.10 ± 0.37	1.04 ± 0.29	1.06 ± 0.24	2.79 ± 0.16	1.73 ± 0.19

Flux values and I_{sc} are in units of $\mu Eq \cdot cm^{-2} \cdot h^{-1}$. GSNO (100 μM) was added bilaterally, and DIDS (50 μM) was added basolaterally. Each unidirectional flux was obtained from four experiments, while net fluxes and I_{sc} were obtained from eight experiments.

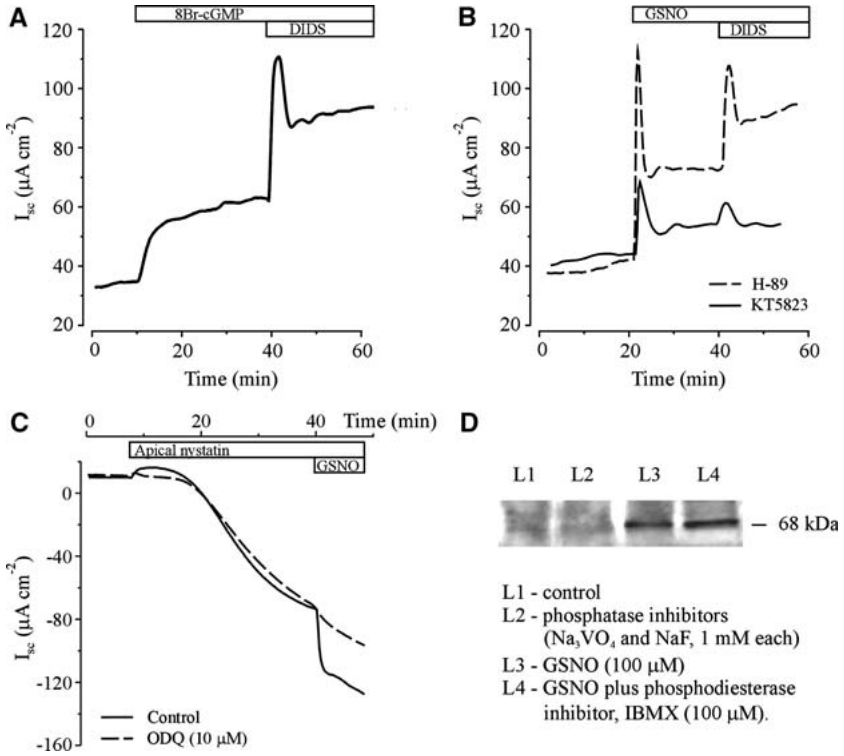

Fig. 5. Basolateral Cl^- channels are activated via a cGMP-dependent pathway. (*A*) In cells pretreated with 8Br-cGMP (1 mM), there is an enhanced response to basolateral DIDS (50 μM) compared to control cells ($n = 3$). (*B*) Pretreatment of Calu-3 cells with the PKA inhibitor H-89 (bilateral, 10 μM) had no significant effect on GSNO (100 μM) and basolateral DIDS responses ($n = 5$). In contrast, the PKG inhibitor KT5823 (2.5 μM) reduced I_{sc} responses to GSNO and DIDS by 42.6% and 83.3% ($n = 4$), respectively. (*C*) Permeabilization of the apical membrane with nystatin reveals a basolateral Cl^- conductance that can be stimulated by GSNO and inhibited by ODQ. The cells were pretreated with L-NAME (1 mM) to inhibit endogenous NO production and in the presence of ouabain (1 mM) to inhibit the electrogenic Na^+/K^+-ATPase. (*D*) Western blot analysis of the bestrophin immunoprecipitate with phospho-specific antibodies revealed the presence of phosphorylated bestrophin after GSNO treatment. IBMX, 3-isobutyl−1-methylxanthine.

effect of NO on transepithelial anion secretion (Fig. 4B). Under baseline conditions, CFTR-mediated HCO_3^- secretion is about three times greater than Cl^- secretion (Fig. 4A). Initially, GSNO induces a change in the (Cl^-:HCO_3^-) flux ratio, increasing the Cl^- flux ~18 times. Following this initial burst of Cl^- secretion, basolateral Cl^- channels open, prompting a switch in the CFTR-mediated anion secretion from Cl^- to HCO_3^-. Subsequent addition of basolateral DIDS inhibits Cl^- recycling across the basolateral membrane, redirecting Cl^- secretion through CFTR.

Basolateral Cl^- Channels Are Regulated via the NO/cGMP-Dependent Pathway

The role of phosphorylation in the regulation of basolateral Cl^- channels was investigated using a cell membrane-permeable analog of cGMP, 8Br-cGMP. Figure 5A shows that 8Br-cGMP (1 mM, bilateral) increased I_{sc} by 16.3 ± 5.7 $\mu A \cdot cm^{-2}$ ($n = 3$) and DIDS (50 μM, basolateral) further increased I_{sc} by 39.7 ± 11.4 $\mu A \cdot cm^{-2}$. Possible crosstalk between cAMP- and cGMP-activated pathways in basolateral Cl^- channel activation was investigated using a PKA inhibitor, H−89. In the presence of H−89, GSNO increased I_{sc} by 52.9 ± 9.3 $\mu A \cdot cm^{-2}$ and DIDS further increased I_{sc} by 32.1 ± 5.3 $\mu A \cdot cm^{-2}$ ($n = 5$, Fig. 5B), indicating that basolateral Cl^- channels were activated independently of PKA activity. The role of PKG in I_{sc} activation was investigated using KT5823, a specific PKG inhibitor. KT5823 (2.5 μM) reduced I_{sc} responses to GSNO and DIDS by 42.6% and 83.3% ($n = 4$), respectively.

Further characterization of basolateral Cl^- channel activation by NO was performed using apical membrane permeabilization. These experiments were performed in HCO_3^--free KHS, with an apical to basolateral Cl^- gradient (129.1:17.1 mM) and in the

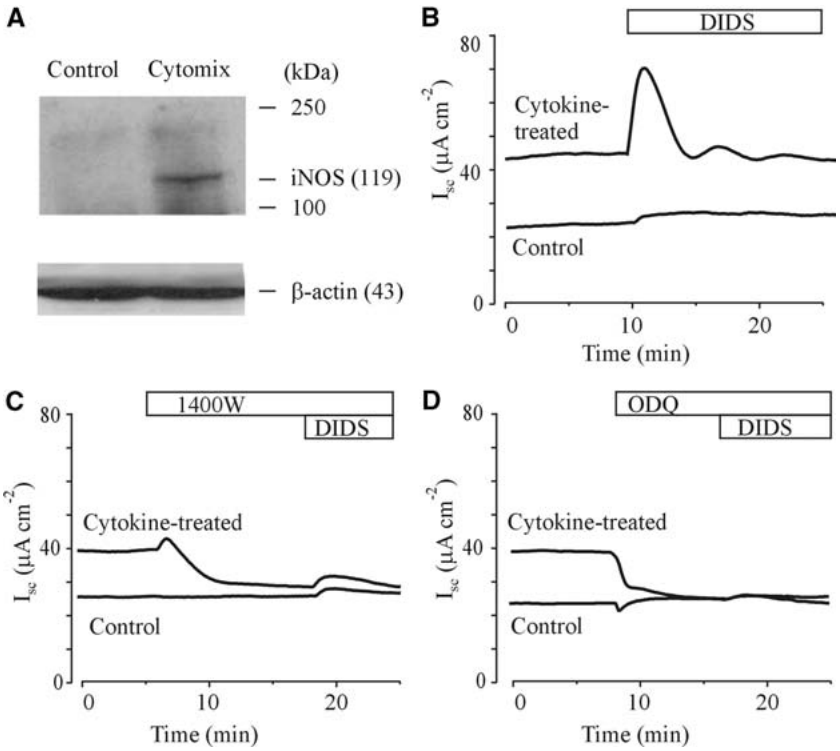

Fig. 6. Cytokine treatment affects iNOS expression and baseline I_{sc}. (*A*) Western blot showing the effect of cytokines (cytomix: TNFα, IFNγ and IL-1β, each at 5 ng/ml) on iNOS expression. iNOS was detected in cytokine-treated, but not in control, Calu-3 cells ($n = 3$ in each set). (*B*) In cytokine-treated cells, basolateral DIDS increased I_{sc} by 26.6 ± 2.4 μA • cm^{-2} ($n = 6$) compared to 2.4 ± 0.3 μA • cm^{-2} ($n = 6$) under control conditions. (*C*) An inhibitor of iNOS, 1400W (20 μM, $n = 3$), inhibited baseline I_{sc} in cytokine-treated cells but had no effect on I_{sc} in control cells. (*D*) An inhibitor of soluble guanylyl cyclase, ODQ (20 μM, $n = 3$), reduced I_{sc} to control levels in cytokine-treated cells but had no effect on I_{sc} in control cells. In the presence of 1400W or ODQ, DIDS (50 μM) did not activate I_{sc} ($n = 3$ in each set, $P > 0.05$, *C* and *D*).

presence of ouabain (1 mM), to inhibit the electrogenic Na^+/K^+-ATPase. Basolateral Na^+-K^+–$2Cl^-$ and Na^+-HCO_3^- cotransporters were inhibited by furosemide (1 mM) and HCO_3^- removal, respectively. Under these conditions, apical nystatin (90 μg/ml) evoked a strong increase in I_{sc}, revealing a basolateral Cl^- conductive pathway (Fig. 5C). While GSNO further increased the basolateral Cl^- current, this effect could be inhibited by ODQ, indicating that basolateral Cl^- channels were activated via a NO/cGMP-dependent pathway. DIDS decreased the peak of GSNO-activated I_{sc} by 39.1 ± 11.9 μA · cm^{-2} ($n = 3$) and by 25.9 ± 7.5 μA · cm^{-2} in the presence of ODQ ($n = 3$, $P < 0.05$, Student's *t*-test).

Bestrophin Functions as a NO-Activated Basolateral Cl^- Channel in Calu–3 Cells

The presence of bestrophin Cl^- channels in the basolateral membrane of Calu–3 cells was demonstrated earlier (Duta et al., 2004). Here, we investigated the effect of GSNO on bestrophin activity using coimmunoprecipitation techniques. Bestrophin was precipitated from control and GSNO-treated cells using bestrophin-specific antibodies, and then precipitates were probed with phospho-specific monoclonal antibodies. Figure 5D shows that under control conditions bestrophin was not phosphorylated (lanes L1 and L2) but became phosphorylated after GSNO treatment (lanes L3 and L4). These results suggest that bestrophin phosphorylation may play a major role in the regulation of basolateral conductance by NO.

Cytokine-Induced NO Activates Basolateral Cl^- Channels

Under baseline conditions, iNOS is not detected in Calu–3 cells (Fig. 6A). However, iNOS can be induced by incubating cells with a mixture of cytokines (TNFα, IFNγ and IL–1β, each at 5 ng/ml) for 12 h. This treatment has no apparent effect on transepithelial resistance (277.8 ± 34.7 Ω/cm^2 and 270.3 ± 11.3 Ω/cm^2 in control [$n = 3$] and cytokine-treated [$n = 12$] cells, respectively) but increases baseline I_{sc} from 36.8 ± 4.4 μA · cm^{-2} in control to 48.3 ± 2.5 μA · cm^{-2} in cytokine-treated cells ($P < 0.01$, *t*-test). The increase in baseline I_{sc} in cytokine-treated cells is probably related to iNOS expression since 1400W (20 μM), a specific inhibitor of iNOS (Garvey et al., 1997), had no effect on I_{sc} in control cells but reduced I_{sc} in cytokine-treated cells to control level (Fig. 6C, $n = 3$, $P < 0.005$). The baseline I_{sc} in cytokine-treated cells was also reduced to control level by an inhibitor of soluble guanylyl cyclase, ODQ (Fig. 6D). DIDS (50 μM, basolateral) increased I_{sc} by 26.6 ± 2.4 μA · cm^{-2} ($n = 6$) in cytokine-treated cells compared to 2.4 ± 0.3 μA · cm^{-2} ($n = 6$) under control conditions (Fig. 6B). The effect of DIDS on I_{sc} activation in cytokine-treated cells, in the presence of either 1400W or ODQ, was not different from DIDS effects on

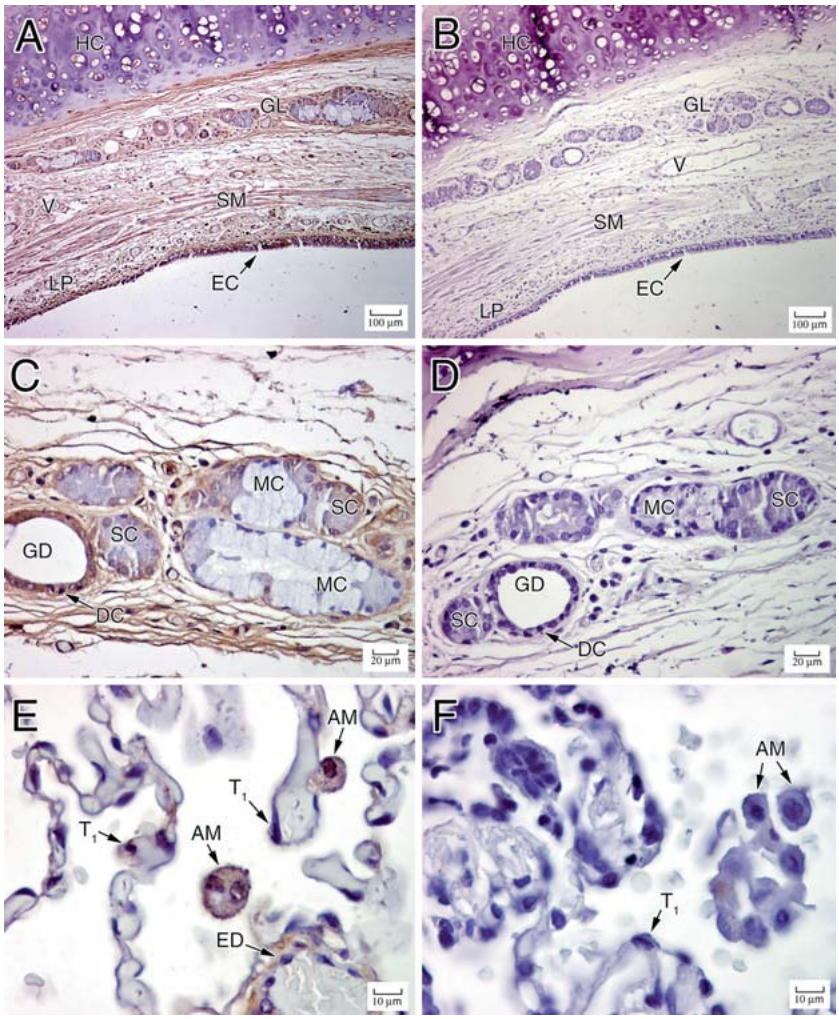

Fig. 7. Bestrophin is expressed in human lung. Immunohistochemistry of normal human lung sections using bestrophin antibody (*A, C, E*) and corresponding isotype controls (mouse IgG; *B, D, F*). (*A, B*) Segmental bronchus (×100). EC, surface epithelium; HC, hyaline cartilage; LP, lamina propria; SM, smooth muscle cell; GL, submucosal gland; V, blood vessel. (*C, D*) Submucosal glands (×400). DC, ductal cell; GD, glandular duct; MC, mucous cell; SC, serous cells. (*E, F*) Small airways and alveoli (×1,000). AM, alveolar macrophage; ED, endothelial cell; T_1, type I cells.

baseline I_{sc} in control cells ($n = 3$ in each set, $P > 0.05$, ANOVA).

Expression of Bestrophin Cl^- Channels in Human Lung

While expression of bestrophin in tissues such as RPE is well documented, little is known about its presence in other tissues. In our previous study, we showed that bestrophin is present in airway epithelial cells using reverse-transcription polymerase chain reaction and Western blot (Duta et al., 2004). Here, we used immunohistochemistry to investigate bestrophin distribution in human lung (Fig. 7). Specific staining for bestrophin was present in airway epithelial cells (Fig. 7A), serous cells of submucosal glands (Fig. 7C) and alveolar macrophages (Fig. 7E). The corresponding isotype control is shown in Figure 7B, D and F. Positive staining for bestrophin was found also in endothelial cells and smooth muscle cells (Fig. 7A). Interestingly, type I pneumocytes (Fig. 7E), type II pneumocytes and mucous cells of submucosal glands (Fig. 7C) did not show any bestrophin expression.

Discussion

NO is present in the parts per billion range in exhaled breath in humans (Leone et al., 1994), but its physiological role in the respiratory system is uncertain (Ricciardolo et al., 2004). The results of our study show that NO is a potent activator of basolateral Cl^- channels in airway epithelial cells, especially under inflammatory conditions, when increased expression of iNOS leads to generation of large amounts of NO. This effect may reduce Cl^- secretion across the apical membrane because of increased Cl^- back-flux across the basolateral membrane.

Biological actions of NO are usually classified as either cGMP-dependent or -independent (Ricciardolo et al., 2004), but many cell types appear to use both pathways (Chen et al., 2006; Gaston et al., 1994). The results of this study indicate that basolateral Cl^- conductance in Calu−3 cells could be activated via the NO/cGMP-dependent pathway. This conclusion is supported by experiments showing that (1) 8Br-cGMP exerted a similar effect on I_{sc} as NO donors; (2) the effect of NO could be completely blocked by an inhibitor of soluble guanylyl cyclase; (3) a specific

inhibitor of PKG, KT5823, reduced the I_{sc} response to basolateral DIDS; and (4) phospho-specific antibodies detected bestrophin in GSNO-treated, but not in control, immunoprecipitates.

The sustained electrogenic Cl^- secretion in epithelia can only result from effects exerted at both the apical and basolateral poles of the epithelial cells. NO donors produce a transient increase in Cl^- secretion, suggesting involvement of additional regulatory mechanisms. Recently, GSNO has been shown to activate apically located CFTR via both cGMP-dependent and cGMP-independent mechanisms (Chen et al., 2006). Another study suggested that GSNO may also exert inhibitory effects on CFTR channel activity by glutathionylation of cys-1344 in the second nucleotide binding domain of human CFTR (Wang et al., 2005). While the complex regulation of CFTR Cl^- channel activity by GSNO may contribute to a transient I_{sc} response, this effect alone is insufficient to explain the stimulatory effects of basolateral Cl^- channel blockers on I_{sc} following GSNO treatment.

The results of our study suggest another hypothesis of GSNO action in airway epithelial cells, based on differential activation of Cl^- channels in the apical and basolateral membranes. Simultaneous measurements of I_{sc} and $^{36}Cl^-$ flux suggest that the delay in the activation of transport processes in the apical and basolateral membranes may be responsible for the transient increase in I_{sc} following NO treatment. GSNO may first activate CFTR in the apical membrane, which leads to an increase in I_{sc}, and then the basolateral Cl^- channels, which causes a decrease in I_{sc}. This hypothesis is in agreement with the results showing that GSNO stimulates transient Cl^- secretion, followed by sustained HCO_3^- secretion and reduced J^{Cl}_{Net} (Fig. 4A, Table 1). It is also supported by measurements showing that DIDS increases J^{Cl}_{Net} by increasing J^{Cl}_{BA} and decreasing Cl^- back-flux (J^{Cl}_{AB}) across the basolateral membrane (Fig. 4A, Table 1). A model of transepithelial anion transport that includes major channels and transporters identified in airway epithelial cells is shown in Figure 4B.

At the present time, two types of Cl^- channels have been identified in the basolateral membrane of epithelial cells, ClC-2 (Catalan et al., 2004; Zdebik et al., 2004) and bestrophin (Duta et al., 2004). ClC-2 channels are insensitive to cyclic nucleotide-dependent phosphorylation, are blocked by Zn^{2+} but not by DIDS and have conductance 2–3 pS (Jentsch et al., 2002). Since GSNO increased basolateral membrane Cl^- conductance in the presence of Zn^{2+} ions, ClC-2 channels are unlikely to play a role in NO-dependent regulation of basolateral membrane Cl^- conductance. On the other hand, bestrophin is highly sensitive to DIDS (Sun et al., 2002) and contains three potential phosphorylation sites for cGMP-dependent protein kinase in the cytoplasmic C-terminal region (Blom et al., 1999). Thus, bestrophin Cl^- channels are likely to play a major role in NO-dependent regulation of transepithelial Cl^- secretion.

Immunohistochemistry studies indicate that bestrophin is present in a number of different cell types in human lung, including surface epithelial cells and serous cells of submucosal glands. Positive staining for bestrophin was found also in alveolar macrophages, endothelial cells and smooth muscle cells but not in type I or type II pneumocytes or in mucous cells of submucosal glands. The function of bestrophin in cells such as alveolar macrophages or smooth muscle cells remains to be established.

In conclusion, our studies show that basolateral Cl^- channels are activated by NO and regulate anion secretion in Calu-3 cells. It is likely that bestrophin Cl^- channels play a major role in this process. These results may also be relevant to the function of RPE since this tissue is the main site of bestrophin expression (Petrukhin et al., 1998) and generates NO in response to a number of cytokines (Goureau, Hicks & Courtois, 1994). NO is believed to help maintain the integrity of the blood-retinal barrier, improving visual acuity (Zech et al., 1998); and this function could be accomplished, in part, through modulation of bestrophin activity.

This work was supported by the Canadian Cystic Fibrosis Foundation and the Canadian Institutes of Health Research.

References

Asano, K., Chee, C.B.E., Gaston, B., Lilly, C.M., Gerard, C., Drazen, J.M., Stamler, J.S 1994. Constitutive and inducible nitric oxide synthase gene expression, regulation, and activity in human lung epithelial cells. *Proc. Natl. Acad. Sci. USA* **91:**10089–10093

Blom, N., Gammeltoft, S., Brunak, S 1999. Sequence and structure-based prediction of eukaryotic protein phosphorylation sites. *J. Mol. Biol.* **294:**1351–1362

Catalan, M., Niemeyer, M.I., Cid, L.P., Sepulveda, F.V 2004. Basolateral ClC-2 chloride channels in surface colon epithelium: Regulation by a direct effect of intracellular chloride. *Gastroenterology* **126:**1104–1114

Chen, L., Patel, R.P., Teng, X., Bosworth, C.A., Lancaster, J.R. Jr., Matalon, S 2006. Mechanisms of cystic fibrosis transmembrane conductance regulator activation by s-nitrosoglutathione. *J. Biol. Chem.* **281:**9190–9199

Devor, D.C., Singh, A.K., Lambert, L.C., DeLuca, A., Frizzell, R.A., Bridges, R.J 1999. Bicarbonate and chloride secretion in Calu−3 human airway epithelial cells. *J. Gen. Physiol.* **113:**743–760

Duszyk, M 2001. Regulation of anion secretion by nitric oxide in human airway epithelial cells. *Am. J. Physiol.* **281:**L450–L457

Duta, V., Szkotak, A.J., Nahirney, D., Duszyk, M 2004. The role of bestrophin in airway epithelial ion transport. *FEBS Lett.* **577:**551–554

Furst, J., Schedlbauer, A., Gandini, R., Garavaglia, M.L., Saino, S., Gschwentner, M., Sarg, B., Lindner, H., Jakab, M., Ritter, M., Bazzini, C., Botta, G., Meyer, G., Kontaxis, G., Tilly, B.C.,

Konrat, R., Paulmichl, M 2005. $ICln_{159}$ folds into a pleckstrin homology domain-like structure. Interaction with kinases and the splicing factor LSm4. *J. Biol. Chem.* **280:**31276–31282

Gallemore, R.P., Hughes, B.A., Miller, S.S 1997. Retinal pigment epithelial transport mechanisms and their contributions to the electroretinogram. *Prog. Retinal Eye Res.* **16:**509–566

Garvey, E.P., Oplinger, J.A., Furfine, E.S., Kiff, R.J., Laszlo, F., Whittle, B.J., Knowles, R.G 1997. 1400W is a slow, tight binding, and highly selective inhibitor of inducible nitric-oxide synthase in vitro and in vivo. *J. Biol. Chem.* **272:**4959–4963

Gaston, B., Drazen, J.M., Jansen, A., Sugarbaker, D.A., Loscalzo, J., Richards, W., Stamler, J.S 1994. Relaxation of human bronchial smooth muscle by S-nitrosothiols in vitro. *J. Pharmacol. Exp. Ther.* **268:**978–984

Goureau, O., Hicks, D., Courtois, Y 1994. Human retinal pigmented epithelial cells produce nitric oxide in response to cytokines. *Biochem. Biophys. Res. Commun.* **198:**120–126

Gyomorey, K., Yeger, H., Ackerley, C., Garami, E., Bear, C.E 2000. Expression of the chloride channel ClC-2 in the murine small intestine epithelium. *Am. J. Physiol.* **279:**C1787–C1794

Hwang, T.H., Lee, H.J., Lee, N.K., Choi, Y.C 2000. Evidence for basolateral but not apical membrane localization of outwardly rectifying depolarization-induced Cl^- channel in airway epithelia. *J. Membr. Biol.* **176:**217–221

Jentsch, T.J., Stein, V., Weinreich, F., Zdebik, A.A 2002. Molecular structure and physiological function of chloride channels. *Physiol. Rev.* **82:**503–568

Kamosinska, B., Radomski, M.W., Duszyk, M., Radomski, A., Man, S.F 1997. Nitric oxide activates chloride currents in human lung epithelial cells. *Am. J. Physiol.* **272:**L1098–L1104

Lane, C., Knight, D., Burgess, S., Franklin, P., Horak, F., Legg, J., Moeller, A., Stick, S 2004. Epithelial inducible nitric oxide synthase activity is the major determinant of nitric oxide concentration in exhaled breath. *Thorax* **59:**757–760

Leone, A.M., Gustafsson, L.E., Francis, P.L., Persson, M.G., Wiklund, N.P., Moncada, S 1994. Nitric oxide is present in exhaled breath in humans: Direct GC-MS confirmation. *Biochem. Biophys. Res. Commun.* **201:**883–887

Marquardt, A., Stohr, H., Passmore, L.A., Kramer, F., Rivera, A., Weber, B.H 1998. Mutations in a novel gene, *VMD2*, encoding a protein of unknown properties cause juvenile-onset vitelliform macular dystrophy (Best's disease). *Hum. Mol. Genet.* **7:**1517–1525

Mummery, J.L., Killey, J., Linsdell, P 2005. Expression of the chloride channel CLC-K in human airway epithelial cells. *Can. J. Physiol. Pharmacol.* **83:**1123–1128

Murray, C.B., Chu, S., Zeitlin, P.L 1996. Gestational and tissue-specific regulation of C1C-2 chloride channel expression. *Am. J. Physiol.* **271:**L829–L837

Petrukhin, K., Koisti, M.J., Bakall, B., Li, W., Xie, G., Marknell, T., Sandgren, O., Forsman, K., Holmgren, G., Andreasson, S., Vujic, M., Bergen, A.A., McGarty-Dugan, V., Figueroa, D., Austin, C.P., Metzker, M.L., Caskey, C.T., Wadelius, C 1998. Identification of the gene responsible for Best macular dystrophy. *Nat. Genet.* **19:**241–247

Qu, Z., Fischmeister, R., Hartzell, C 2004. Mouse bestrophin-2 is a bona fide Cl^- channel: Identification of a residue important in anion binding and conduction. *J. Gen. Physiol.* **123:**327–340

Ricciardolo, F.L.M., Sterk, P.J., Gaston, B., Folkerts, G 2004. Nitric oxide in health and disease of the respiratory system. *Physiol. Rev.* **84:**731–765

Sanders, E.J., Parker, E 2002. The role of mitochondria, cytochrome *c* and caspase-9 in embryonic lens fibre cell denucleation. *J. Anat.* **201:**121–135

Seidler, U., Blumenstein, I., Kretz, A., Viellard-Baron, D., Rossmann, H., Colledge, W.H., Evans, M., Ratcliff, R., Gregor, M 1997. A functional CFTR protein is required for mouse intestinal cAMP-, cGMP- and Ca^{2+}-dependent HCO_3^- secretion. *J. Physiol.* **505:**411–423

Schultz, S.G., Zalusky, R 1964. Ion transport in isolated rabbit ileum. *J. Gen. Physiol.* **47:**567–584

Sun, H., Tsunenari, T., Yau, K.W., Nathans, J 2002. The vitelliform macular dystrophy protein defines a new family of chloride channels. *Proc. Natl. Acad. Sci. USA* **99:**4008–4013

Szkotak, A.J., Man, S.F.P., Duszyk, M 2003. The role of the basolateral outwardly rectifying chloride channel in human airway epithelial anion secretion. *Am. J. Respir. Cell Mol. Biol.* **29:**710–720

Wang, W., Oliva, C., Li, G., Holmgren, A., Lillig, C.H., Kirk, K.L 2005. Reversible silencing of CFTR chloride channels by glutathionylation. *J. Gen. Physiol.* **125:**127–141

Willumsen, N.J., Davis, C.W., Boucher, R.C 1989. Intracellular Cl^- activity and cellular Cl^- pathways in cultured human airway epithelium. *Am. J. Physiol.* **256:**C1033–C1044

Zdebik, A.A., Cuffe, J.E., Bertog, M., Korbmacher, C., Jentsch, T.J 2004. Additional disruption of the ClC-2 Cl^- channel does not exacerbate the cystic fibrosis phenotype of cystic fibrosis transmembrane conductance regulator mouse models. *J. Biol. Chem.* **279:**22276–22283

Zech, J.C., Pouvreau, I., Cotinet, A., Goureau, O., Le Varlet, B., Kozak, Y 1998. Effect of cytokines and nitric oxide on tight junctions in cultured rat retinal pigment epithelium. *Invest. Ophthalmol. Vis. Sci.* **39:**1600–1608